Astron. Astrophys. 237, 23–35 (1990)

ASTRONOMY AND ASTROPHYSICS

# Optical HII regions in NGC 2403*

**J.-P. Sivan[1], H. Petit[2], G. Comte[2], and A.J. Maucherat[1]**

[1] Laboratoire d'Astronomie Spatiale du CNRS, Les Trois Lucs, F-13012 Marseille, France
[2] Observatoire de Marseille, 2 place Le Verrier, F-13248 Marseille Cedex 04, France

Received April 2; accepted May 21, 1990

**Abstract.** The distribution of the ionized hydrogen in the spiral galaxy NGC 2403 is studied from Hα narrow-band photographs taken with the soviet 6-meter telescope. A catalogue of 366 HII regions has been compiled: it lists $X, Y$ offset positions, absolute Hα fluxes and angular diameters corrected for instrumental broadening. It is found that the frequency distribution of the HII region diameters follows van den Bergh's law and that the Hα luminosity function is well represented by a power-law. The study of the spatial distribution of the HII regions in the galactic plane does not reveal any conspicuous regular spiral pattern. The rate of massive star formation, as deduced from the ratio of the Hα intrinsic flux to the projected mean surface density of hydrogen, is found to be regularly decreasing from the center to the exterior of the galaxy. But the ratio of the Hα flux to the near-ultraviolet luminosity indicates that beyond 9′ from the center, the galaxy gradually becomes unable to form very massive stars, thus suggesting that the Initial Mass Function should be truncated there at a lower mass cutoff than in the central regions.

Spectrophotometric data are presented for 52 HII regions and 7 directions in the diffuse ionized background. The $N^+/S^+$ abundance gradient calculated from all the regions observed spectrophotometrically is in agreement with previous determinations. Also, the SII lines at 6717 and 6731 Å are found significantly brighter in the diffuse background than in the *classical* HII regions, as previously found in the arms of our Galaxy.

**Key words:** galaxies: NGC 2403 – galaxies: structure of – interstellar medium: abundances – interstellar medium: HII regions: general – luminosity function, mass function – stars: formation of

## 1. Introduction

Several years ago, a program of Hα narrow-band photography of HII regions in galaxies was undertaken at the 6-meter telescope of the Special Astrophysical Observatory in Zelentchuk (USSR) with an $f/1$ focal reducer (Courtès et al., 1987). Several galaxies have been surveyed: NGC 6946 (Bonnarel et al., 1986), M 33 (Courtès et al., 1987), M 81 (Petit et al., 1988) and NGC 2403 to which this paper is devoted.

NGC 2403 is a bright spiral classified SAB(s)cd III by de Vaucouleurs et al. (1976) and Sc(s) III by Sandage and Tammann (1981). On large-scale blue photographs, it looks very much like M 33 and NGC 300, of very similar types and luminosity classes. It is generally said to belong to the M 81 Group (but some authors invoke the splitting of this group in two subgroups, NGC 2403 belonging to the closest one) and estimates of its distance range from 2.6 to 3.4 Mpc. NGC 2403 has been the subject of numerous studies from X-rays to radio frequencies. Surface photometry in B and V bands has been published by Okamura et al. (1977) who discovered a *blue ring* between 2 and 4′ from the center, supposed to be the trace of an active zone of recent star formation. The neutral hydrogen distribution was first studied by Shostak and Rogstad (1973) and Shostak (1973) and then, with much improved resolution, by Wevers (1984), who complemented the HI data with a surface photometry in ultraviolet and red.

Optical HII regions have been catalogued and/or mapped by Véron and Sauvayre (1965), Hodge (1969), Lynds (1974) and Hodge and Kennicutt (1983a). In these papers, neither fluxes nor dimensions are given for the identified regions. Spectrophotometry has been obtained for some of them by Smith (1975), Jensen et al. (1976), McCall et al. (1985) and Fierro et al. (1986). Physical parameters, excitation conditions and chemical abundance are studied by these authors. However only the brightest regions have been studied.

In this paper, we present a catalogue of 366 HII regions, with, for each of them, accurate positions, integrated Hα fluxes and angular diameters and, for 52 of them, the $H\alpha/[NII]$ and $[NII]/[SII]$ line intensity ratios. These ratios have also been measured on the diffuse ionized medium outside the *classical* localized HII regions. Although these spectrophotometric data concern only three emission lines, they are of interest because the line intensities are measured on a large sample of HII regions and on much fainter, diffuse emission regions where it has been found, for our Galaxy, that the above ratios are significantly different (Reynolds, 1989).

In Section 2 we present the observational material and in Section 3 we describe the data reduction procedure. The catalogue is given in Section 4. The data are discussed in Section 5 in terms of frequency distribution of diameters, luminosity function, spatial distribution across the disk of the galaxy, nitrogen to sulfur abundance gradient and excitation conditions

*Send offprint requests to*: J.-P. Sivan

* Based on observations collected at the Special Astrophysical Observatory (URSS) and at the Observatoire de Haute Provence du CNRS

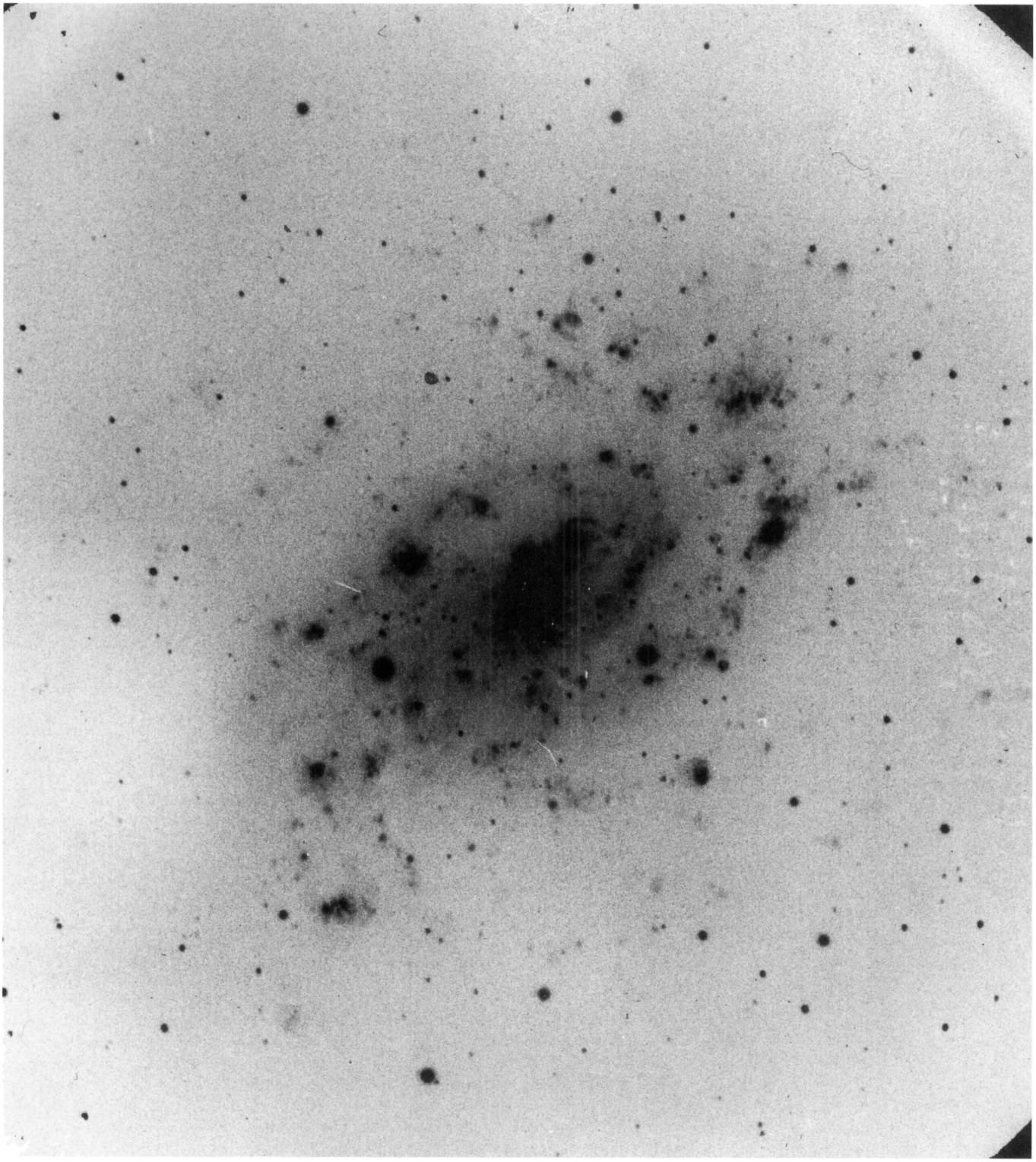

**Fig. 1a.** f/1 narrow-band Hα photograph of NGC 2403 obtained at the prime focus of the 6-m telescope in Zelentchuk (190-min exposure on Kodak 103 aE film).

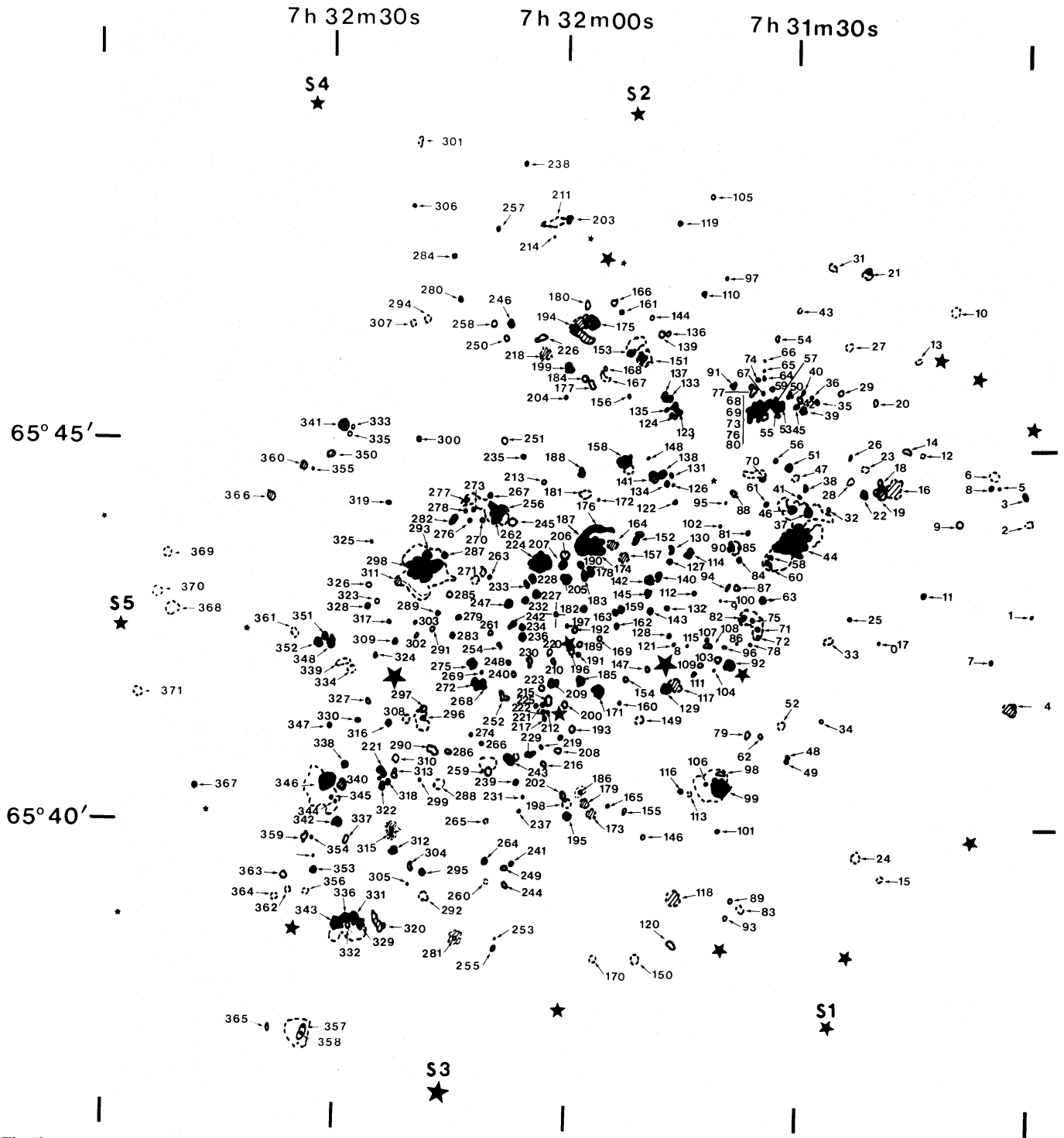


**Fig. 1b.** Identification chart for the 366 HII regions detected in Fig. 1a (1950.0 equatorial coordinates).

of the ionized gas, and radial behaviour of the rate of formation of massive stars.

## 2. Observational material

### *2.1. Hα photographs*

Three Hα photographs of NGC 2403 were obtained at the prime focus of the 6-m telescope equiped with the $f/1$ focal reducer of Courtès: a 195-min (Fig.1a) exposure centered on the galaxy center and 60-min and 180-min exposures centered 01 min 00 s east and 01′ 08″ south of the galaxy center. All exposures are on pre-flashed Kodak 103 aE film. The field is 20′ in diameter and the scale is 34″.4 $mm^{-1}$. The angular resolution is limited by the seeing to about 1″. The interference filter is centered at 6552 Å and is 35 Å wide (FWHM) so that the shifted wavelength of the Hα line is always above 50% transmission. The limiting

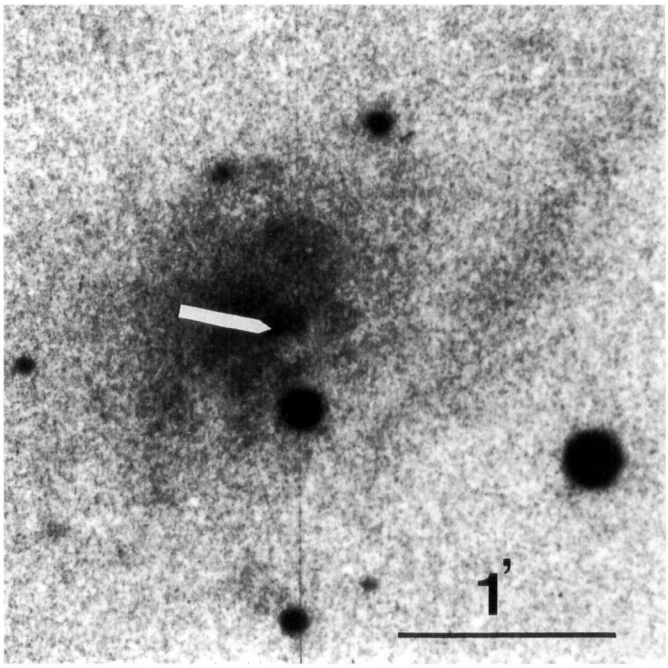


**Fig. 2.** Central part of a comparison photograph of NGC 2403 obtained in the continuum adjacent to Hα at the 1.2-m telescope of the Observatoire de Haute Provence: the white arrow shows the nucleus of the galaxy, whose equatorial coordinates (given in the text) are those of the center of the $X,Y$ reference frame of the identified HII regions in NGC 2403. North is at the top and east is to the left.

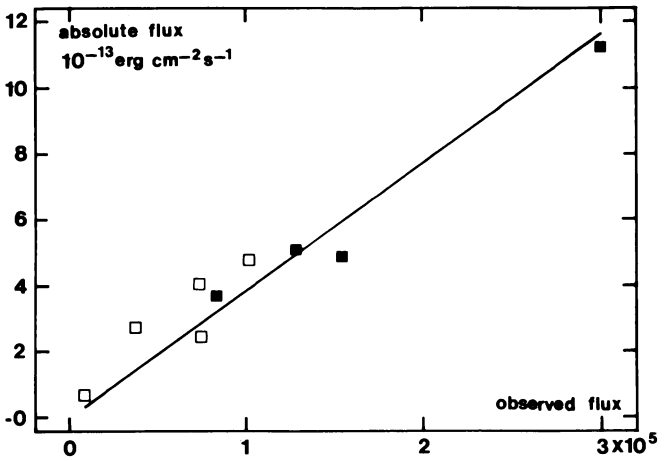


**Fig. 3.** Absolute flux calibration: absolute Hα fluxes from the literature versus Hα fluxes measured on our plates (instrumental arbitrary units). Filled squares are for regions from Fierro et al. (1986), empty squares for regions from McCall et al. (1985). The regression line gives $F(H\alpha)$ ($10^{-16}$erg cm$^{-2}$ s$^{-1}$) = (0.039±0.003) $\times f_{observed}$ (instrumental units).

Hα surface brightness of the longest exposures is estimated at $4\,10^{-6}$ erg cm$^{-2}$ s$^{-1}$ sr$^{-1}$. A comparison photograph (Fig. 2) was obtained in the continuum adjacent to Hα at the 1.2-m telescope of the Observatoire de Haute Provence. Also at our disposal was a grism plate obtained by J.Lequeux at the Canada France Hawai 3.6-m telescope.

### 2.2. *Spectrophotometry*

The observations were carried out with the Cassegrain Nebular Spectrograph of the 1.93-m telescope of the Observatoire de Haute Provence (Deharveng and Pellet, 1970). The observational procedure has been fully described by Comte and Monnet (1974). Nine spectra were obtained for different slit positions across the galaxy, between 6450 and 6800 Å, with a resolution of 4 Å. The spectra were photographed on baked Kodak IIaO plates from the phosphor screen of an RCA magnetically focussed image-tube intensifier. The projected slit on the sky was 7′ in length and 7″.7 in width. This allowed us to observe a total of 52 individual HII regions and some regions of diffuse emission.

## 3. Data Reduction

### 3.1. *Hα photographs*

A preliminary identification of the HII regions was carefully conducted by visual intercomparison of the Hα photographs, the continuum photograph and the grism. This permitted the rejection of foreground stars and gelatine defects. The Hα photographs were then digitized with the PDS microdensitometer of the Laboratoire d'Astronomie Spatiale using a 20$\mu m$ square scanning slit and a 20$\mu m$ (= 0″7) sampling step. The data reduction was performed partly on the VAX computer of the Observatoire de Marseille and on that of the Laboratoire d'Astronomie Spatiale, using MIDAS procedures and special procedures designed in the framework of MIDAS. The method was the same as that used for M 81 (Petit et al., 1988). It can be summarized as follows:

- The photographic densities were converted into arbitrary intensities using a relative photometric calibration of the emulsion.
- Isophotal contours of the identified regions, drawn interactively, allowed us to confirm the preliminary identification and sometimes led us to slightly modify it.
- We assigned to each region the $X, Y$ positions of the photometric center of the corresponding isophotal system. The $X, Y$ coordinates, measured in the PDS reference frame, were then converted to a system centered on the galaxy center, with the $X$ and $Y$ axes in the E-W and N-S directions respectively. The $X, Y$ center of the galaxy was determined in the continuum photograph (Fig. 2) and the coordinates were reduced with the astrometric star positions given by Wevers (1984). The uncertainty is estimated to be lower than 1″ for the $X, Y$ offset positions.
- The flux was computed for each region by interactive integration of the intensity contained within the outermost isophote down to the local threshold and corrected for the background intensity.
- A tentative absolute calibration of the Hα fluxes was derived from published spectrophotometric results in the following way:
  1) Absolute brightnesses in Hβ line are given by McCall et al. (1985) for 5 HII regions of our sample (the far outlying object Hodge 109 is located beyond the limits of our field). The spectrograph slits used by these authors range in size from 3″.9 × 4″ to 4″ × 7″.4 (see McCall 1982).

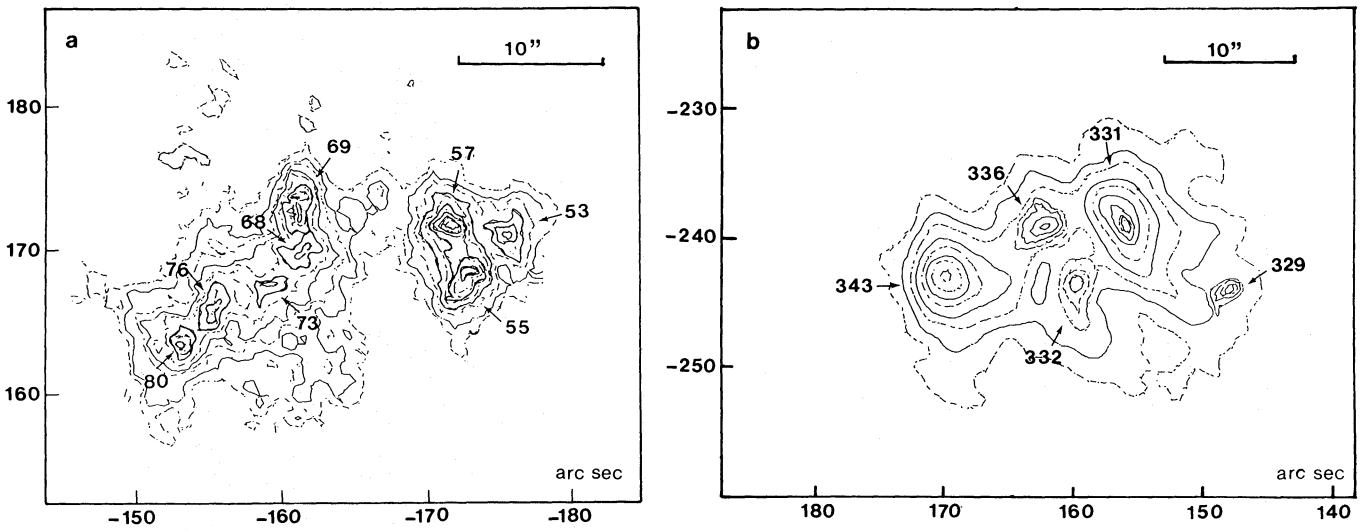


**Fig. 4.** Identifying HII regions in NGC 2403: contour maps of two bright Hα emission complexes (the numbers refer to the catalogue of Table 1).

We therefore assumed that: i) their brightness figure is valid for a 4″.65 × 4″.65 square aperture, which, projected on our plates, encompasses 9 × 9 pixels on the digitized image, ii) this brightness figure is an average value valid for the brightest part of the HII region.

2) Absolute Hβ fluxes are given by Fierro et al. (1986) as observed through a rectangular aperture of size 3″.8 × 12″.4, which, projected on our plates, encompasses 24 × 7.5 pixels on the digitized images. Again it was assumed that these values referred to the slit centered on the brightest part of the HII region .
3) Instrumental fluxes inside the simulated apertures were then computed and compared with the absolute Hα fluxes: these were derived from the Hβ data and the observed $H\alpha/H\beta$ intensity ratio. The adopted calibration is shown in Fig. 3.

- We measured for each region an *effective diameter D*, following the method of Milliard and Marcelin (1981):
$D = 2k\,(A_2 - A_2^*)^{1/2}/\sqrt{\pi}$,
where k is a scale factor, and $A_2$ and $A_2^*$ are the film areas containing half the total flux, respectively for the HII region and for a field star of the same total flux.
- Most of the measurements were performed on the two long-exposure photographs. The short one was used for the brightest regions in the innermost part of the galaxy which are overexposed on the long exposures. The difficulty in identifying and measuring HII regions in large bright complexes has been fully discussed by Kennicutt (1979). As an illustration to our work, we show in Fig. 4 the Hα contour map we obtained for the emission complexes lying at $X = -161''$, $Y = 170''$ and $X = 160''$, $Y = -244''$.

### 3.2. Spectrophotometry

The reduction procedure was the same as that used by Comte and Monnet (1974). Photometric calibration was based on the ratio $I([NII]\lambda6584)/I([NII\lambda6548)$ measured in spectra of galactic HII regions.(The value of this ratio is known to be constant and equal to 3.0).

Hα, [NII]λ6548, [NII]λ6584, [SII]λ6717 and [SII]λ6731 line intensities were obtained for 52 identified HII regions and for 7 directions in the Hα diffuse background, with a spatial resolution of 10″ × 7″.7. (The larger dimension corresponds to the height of the slit of the microphotometer and the other one to the width of the slit of the spectrograph). The error in the line intensity ratios is estimated to be ranging from 10% (well-exposed HII regions) to 30% (faint, diffuse regions).

## 4. The Chart and the Catalogue

A total of 366 regions have been identified. They are shown in the identification chart (Fig. 1b) and listed in Table 1.

The table gives the following information:

- *Column 1* lists the reference number given to individual HII regions as shown in the chart.
- *Columns 2 and 3* give the $X, Y$ positions of the photometric center of the regions, in units of arc sec. The coordinate system is centered on the nucleus of the galaxy: $\alpha_{1950}$ = 07 h 32 min 01.2 s, $\delta_{1950} = 65°42'45''$. (These coordinates were chosen instead of the usually adopted center at 07 h 32 min 01.2 s, 65°42′57″ after careful measurement of the continuum photograph, as indicated in Section 3.1). The $X$-axis is in the E-W direction with negative values to the west and the $Y$-axis is in the N-S direction with negative values to the south.
- *Column 4* lists the total Hα fluxes of the regions in units of $10^{-16}$ erg cm$^{-2}$ s$^{-1}$.
- *Column 5* gives the *effective* (half-flux) diameters $D$ as defined in Section 3.1 in units of $10^{-1}$ arcsec. An asterisk (*) indicates that the region is not resolved.
- *Columns 6 and 7* give respectively the logarithm of the $I(H\alpha)/I([NII]\lambda6584)$ line intensity ratio and the logarithm of the $I([NII]\lambda6548+6584)/I([SII]\lambda6717+6731)$ ratio for the regions observed spectrophotometrically. The [NII]λ6548 line is generally very faint and blended with nightsky lines: we have prefered to take $I([NII]\lambda6548 + 6584) = 1.33\,I([NII]\lambda6584)$.

**Table 1.** Catalogue of HII regions in NGC2403

| # | X (arcsec) | Y (arcsec) | Hα FLUX ($10^{-16}$erg cm$^{-2}$s$^{-1}$) | DIAMETER ($10^{-1}$arcsec) | log Hα/[NII]6584 | log [NII]/[SII] |
|---|---|---|---|---|---|---|
| 1 | -376. | 5. | 14. | * | * | * |
| 2 | -374. | 78. | 50. | 42. | * | * |
| 3 | -371. | 100. | 91. | 33. | * | * |
| 4 | -363. | -66. | 161. | 78. | * | * |
| 5 | -348. | 106. | 7. | 7. | * | * |
| 6 | -347. | 115. | 36. | 40. | * | * |
| 7 | -344. | -32. | 23. | 31. | * | * |
| 8 | -343. | 107. | 63. | 23. | * | * |
| 9 | -318. | 78. | 38. | 48. | * | * |
| 10 | -314. | 244. | 39. | 50. | * | * |
| 11 | -290. | 21. | 27. | 39. | * | * |
| 12 | -288. | 132. | 13. | * | * | * |
| 13 | -284. | 205. | 20. | 25. | * | * |
| 14 | -277. | 133. | 91. | 60. | * | * |
| 15 | -258. | -203. | 12. | * | * | * |
| 16 | -258. | 104. | 66. | 34. | * | * |
| 17 | -255. | -18. | 13. | * | * | * |
| 18 | -253. | 110. | 39. | 37. | * | * |
| 19 | -252. | 100. | 146. | 66. | * | * |
| 20 | -250. | 173. | 75. | 35. | * | * |
| 21 | -244. | 276. | 366. | 64. | * | * |
| 22 | -243. | 100. | 187. | 32. | * | * |
| 23 | -243. | 120. | 14. | 15. | * | * |
| 24 | -239. | -185. | 71. | 53. | * | * |
| 25 | -233. | 2. | 13. | * | * | * |
| 26 | -231. | 130. | 29. | 13. | * | * |
| 27 | -231. | 216. | 58. | 59. | * | * |
| 28 | -231. | 113. | 34. | 40. | * | * |
| 29 | -223. | 180. | 50. | 29. | * | * |
| 31 | -215. | 279. | 66. | 37. | * | * |
| 32 | -214. | 88. | 39. | * | * | * |
| 33 | -214. | -16. | 32. | 45. | * | * |
| 34 | -211. | -80. | 8. | * | * | * |
| 35 | -204. | 173. | 45. | 21. | * | * |
| 36 | -199. | 176. | 26. | 12. | * | * |
| 37 | -198. | 85. | 327. | 20. | 0.80 | -0.22 |
| 38 | -196. | 104. | 73. | 12. | * | * |
| 39 | -194. | 167. | 167. | 27. | * | * |
| 40 | -193. | 178. | 44. | 17. | * | * |
| 41 | -191. | 98. | 34. | * | * | * |
| 42 | -191. | 174. | 68. | 21. | * | * |
| 43 | -190. | 244. | 10. | * | * | * |
| 44 | -190. | 60. | 24442. | 81. | 0.86 | 0.00 |
| 45 | -188. | 169. | 102. | * | * | * |
| 46 | -188. | 88. | 574. | 48. | 0.61 | -0.32 |
| 47 | -188. | 113. | 96. | 52. | * | * |
| 48 | -185. | -108. | 67. | 29. | * | * |
| 49 | -184. | -111. | 71. | 36. | * | * |
| 50 | -183. | 178. | 89. | 29. | * | * |
| 51 | -183. | 120. | 716. | * | * | * |
| 52 | -180. | -85. | 30. | 43. | * | * |
| 53 | -176. | 171. | 227. | 22. | * | * |
| 54 | -173. | 220. | 30. | 16. | * | * |
| 55 | -173. | 168. | 394. | 18. | * | * |
| 56 | -172. | 126. | 21. | * | * | * |
| 57 | -172. | 171. | 430. | 26. | * | * |
| 58 | -169. | 49. | 61. | 10. | * | * |
| 59 | -169. | 181. | 6. | * | * | * |
| 60 | -167. | 44. | 301. | 26. | * | * |
| 61 | -165. | 91. | 25. | 16. | * | * |
| 62 | -165. | -93. | 23. | 18. | * | * |
| 63 | -164. | 16. | 199. | 23. | * | * |
| 64 | -163. | 190. | 28. | 11. | * | * |
| 65 | -163. | 197. | 7. | * | * | * |
| 66 | -163. | 204. | 27. | 17. | * | * |
| 67 | -162. | 179. | 19. | * | * | * |
| 68 | -161. | 170. | 543. | 29. | 0.81 | -0.10 |
| 69 | -161. | 172. | 340. | 15. | * | * |
| 70 | -161. | 111. | 144. | 35. | 0.53 | -0.25 |
| 71 | -160. | -8. | 134. | 41. | * | * |
| 72 | -160. | -13. | 71. | 26. | * | * |
| 73 | -159. | 167. | 253. | * | * | * |
| 74 | -158. | 189. | 27. | * | * | * |
| 75 | -156. | -1. | 116. | 42. | * | * |
| 76 | -155. | 166. | 346. | 14. | * | * |
| 77 | -155. | 179. | 27. | 18. | * | * |
| 78 | -154. | -19. | 25. | 9. | * | * |
| 79 | -153. | -90. | 22. | 23. | * | * |
| 80 | -153. | 163. | 503. | 31. | * | * |
| 81 | -151. | 69. | 17. | 8. | * | * |
| 82 | -149. | 1. | 106. | 28. | * | * |
| 83 | -147. | -229. | 69. | 74. | * | * |
| 84 | -145. | 48. | 144. | 24. | * | * |
| 85 | -144. | 57. | 51. | 19. | * | * |
| 86 | -144. | -19. | 19. | * | * | * |
| 87 | -143. | 26. | 82. | 40. | * | * |
| 88 | -140. | 99. | 64. | 29. | * | * |
| 89 | -140. | -221. | 22. | 74. | * | * |
| 90 | -139. | 57. | 157. | 31. | 0.74 | * |
| 91 | -139. | 185. | 134. | 26. | * | * |
| 92 | -138. | -36. | 1096. | 40. | 0.60 | -0.17 |
| 93 | -136. | -235. | 12. | 6. | * | * |
| 94 | -136. | 25. | 54. | 27. | * | * |
| 95 | -135. | 93. | 12. | * | * | * |
| 96 | -134. | -22. | 15. | * | * | * |
| 97 | -132. | 269. | 73. | 8. | * | * |
| 98 | -131. | -122. | 129. | 43. | * | * |
| 99 | -131. | -136. | 5460. | 41. | * | * |
| 100 | -131. | 14. | 15. | 6. | * | * |
| 101 | -130. | -168. | 26. | 23. | * | * |
| 102 | -129. | 74. | 29. | * | * | * |
| 103 | -128. | -33. | 68. | 44. | * | * |
| 104 | -126. | -46. | 6. | * | * | * |
| 105 | -120. | 332. | 8. | * | * | * |
| 106 | -120. | -130. | 23. | * | * | * |
| 107 | -120. | -16. | 19. | * | * | * |
| 108 | -120. | -21. | 63. | 21. | * | * |
| 109 | -116. | -37. | 53. | 22. | * | * |
| 110 | -114. | 256. | 118. | 21. | * | * |
| 111 | -110. | -44. | 57. | 30. | * | * |
| 112 | -110. | 20. | 43. | 13. | * | * |
| 113 | -108. | -138. | 30. | 16. | * | * |
| 114 | -106. | 51. | 341. | 58. | 0.75 | -0.12 |
| 115 | -105. | -22. | 12. | * | * | * |
| 116 | -101. | -136. | 87. | 12. | * | * |
| 117 | -96. | -56. | 78. | 30. | * | * |
| 118 | -96. | -224. | 105. | 80. | * | * |
| 119 | -95. | 313. | 107. | 1. | * | * |
| 120 | -94. | -257. | 57. | 36. | * | * |
| 121 | -94. | -20. | 38. | * | * | * |
| 122 | -93. | 91. | 90. | 38. | * | * |
| 123 | -93. | 167. | 386. | 46. | * | * |
| 124 | -91. | 161. | 115. | 33. | * | * |
| 126 | -91. | 106. | 37. | 13. | * | * |
| 127 | -90. | 45. | 219. | 61. | 0.80 | -0.12 |
| 128 | -90. | -14. | 164. | 21. | * | * |
| 129 | -90. | -56. | 1293. | 33. | * | * |
| 130 | -89. | 56. | 150. | 64. | 0.65 | -0.04 |
| 131 | -89. | 114. | 62. | 27. | * | * |
| 132 | -88. | 9. | 8. | * | * | * |
| 133 | -88. | 173. | 154. | 15. | 0.52 | -0.21 |
| 134 | -87. | 106. | 132. | 26. | 0.91 | -0.28 |
| 135 | -87. | 165. | 61. | 36. | * | * |
| 136 | -86. | 224. | 17. | 23. | * | * |
| 137 | -84. | 174. | 317. | 40. | 0.52 | -0.21 |
| 138 | -84. | 115. | 354. | 38. | 0.58 | -0.10 |
| 139 | -82. | 223. | 17. | 33. | * | * |
| 140 | -81. | 35. | 457. | 73. | 0.49 | 0.02 |
| 141 | -78. | 111. | 113. | 29. | 0.58 | -0.10 |
| 142 | -75. | 31. | 439. | 67. | * | * |
| 143 | -75. | 6. | 179. | 38. | 0.51 | -0.07 |
| 144 | -74. | 236. | 10. | * | * | * |
| 145 | -73. | 20. | 587. | 62. | 0.59 | 0.17 |
| 146 | -72. | -172. | 6. | * | * | * |
| 147 | -72. | -42. | 52. | * | * | * |
| 148 | -72. | 127. | 15. | * | * | * |
| 149 | -69. | -81. | 56. | 46. | * | * |
| 150 | -67. | -266. | 39. | 56. | * | * |
| 151 | -66. | 205. | 796. | 47. | 0.92 | -0.15 |
| 152 | -66. | 66. | 242. | 23. | 0.68 | 0.31 |
| 153 | -57. | 209. | 297. | 23. | 0.55 | -0.20 |
| 154 | -56. | -48. | 61. | 39. | * | * |
| 155 | -56. | -154. | 46. | 27. | * | * |
| 156 | -56. | 175. | 29. | 17. | * | * |
| 157 | -53. | 47. | 161. | 54. | 0.68 | -0.20 |
| 158 | -53. | 122. | 2689. | 43. | 1.20 | -0.54 |
| 159 | -52. | 8. | 559. | 94. | * | * |
| 160 | -51. | -68. | 74. | 26. | * | * |
| 161 | -50. | 240. | 73. | 4. | * | * |
| 162 | -49. | -7. | 129. | 30. | * | * |
| 163 | -47. | 4. | 562. | 93. | * | * |
| 164 | -45. | 56. | 49. | 32. | * | * |
| 165 | -43. | -148. | 55. | 38. | * | * |
| 166 | -43. | 248. | 36. | 28. | * | * |
| 167 | -41. | 187. | 25. | 33. | * | * |
| 168 | -37. | 197. | 15. | * | * | * |
| 169 | -36. | -17. | 35. | 23. | * | * |
| 170 | -34. | -269. | 47. | 30. | * | * |
| 171 | -34. | -57. | 559. | 54. | 0.83 | 0.16 |
| 172 | -33. | 93. | 23. | * | * | * |
| 173 | -31. | -157. | 100. | 74. | * | * |
| 174 | -29. | 57. | 19819. | 63. | 0.71 | 0.20 |
| 175 | -28. | 233. | 672. | 80. | * | * |
| 176 | -28. | 71. | 235. | 39. | 0.47 | -0.10 |
| 177 | -27. | 182. | 73. | 33. | * | * |
| 178 | -27. | 36. | 477. | 87. | 0.51 | -0.08 |
| 179 | -24. | -145. | 47. | 31. | * | * |
| 180 | -24. | 244. | 7. | * | * | * |
| 181 | -23. | 96. | 279. | 54. | 0.00 | 0.12 |
| 182 | -22. | 6. | 219. | 25. | * | * |
| 183 | -22. | 31. | 360. | 43. | 0.51 | -0.08 |
| 184 | -22. | 189. | 75. | 39. | * | * |
| 185 | -21. | -49. | 197. | 52. | * | * |
| 186 | -21. | -139. | 9. | * | * | * |
| 187 | -20. | 61. | 440. | 37. | * | * |
| 188 | -19. | 114. | 212. | 31. | * | * |
| 189 | -19. | -21. | 218. | 24. | * | * |
| 190 | -19. | 42. | 132. | 22. | 0.75 | -0.07 |
| 191 | -18. | -29. | 38. | 25. | * | * |
| 192 | -15. | -10. | 67. | 12. | * | * |
| 193 | -14. | -89. | 183. | 22. | 1.10 | 0.06 |
| 194 | -13. | 227. | 485. | 30. | * | * |
| 195 | -12. | -157. | 317. | 33. | * | * |
| 196 | -12. | -26. | 140. | 33. | * | * |
| 197 | -9. | -7. | 180. | 46. | * | * |
| 198 | -9. | -143. | 72. | 28. | * | * |
| 199 | -9. | 196. | 881. | 20. | * | * |
| 200 | -8. | -69. | 34. | * | * | * |
| 202 | -7. | -138. | 52. | 29. | * | * |
| 203 | -7. | 313. | 30. | 23. | * | * |
| 204 | -7. | 174. | 18. | * | * | * |
| 205 | -6. | 30. | 703. | 46. | 0.71 | 0.08 |
| 206 | -6. | 49. | 827. | 30. | 0.82 | -0.01 |
| 207 | -4. | 42. | 76. | 30. | 0.68 | 0.02 |
| 208 | -4. | -105. | 97. | 36. | 0.76 | * |
| 209 | 0. | -53. | 373. | 54. | 0.58 | 0.14 |
| 210 | 2. | -34. | 120. | * | * | * |
| 211 | 2. | 308. | 16. | * | * | * |
| 212 | 3. | -76. | 80. | 34. | * | * |
| 213 | 4. | 108. | 30. | 20. | * | * |
| 214 | 4. | 299. | 14. | * | * | * |
| 215 | 4. | -65. | 461. | 58. | 0.83 | -0.21 |

**Table 1.** (continued)

| | | | | | | | | | | | | | | | | | | |
|---|---|---|---|---|---|---|---|---|---|---|---|---|---|---|---|---|---|---|
| 216 | 7. | -115. | 28. | | 22. | * | | * | 293 | 101. | 47. | 138. | | 13. | * | | * | |
| 217 | 9. | -79. | 28. | | 3. | * | | * | 294 | 102. | 233. | 32. | | 26. | * | | * | |
| 218 | 9. | 205. | 86. | | 71. | * | | * | 295 | 102. | -202. | 239. | | 24. | * | | * | |
| 219 | 10. | -101. | 9. | * | | * | | * | 296 | 102. | -81. | 195. | | 24. | * | | * | |
| 220 | 10. | -27. | 53. | * | | * | | * | 297 | 103. | -74. | 75. | | 26. | * | | * | |
| 221 | 10. | -69. | 56. | * | | * | | * | 298 | 104. | 37. | 30010. | | 85. | | 0.94 | | -0.08 |
| 222 | 10. | -74. | 20. | * | | * | | * | 299 | 105. | -128. | 20. | | 22. | * | | * | |
| 223 | 10. | -56. | 68. | | 26. | * | | * | 300 | 109. | 140. | 33. | | 32. | * | | * | |
| 224 | 12. | 43. | 9878. | | 62. | | 0.74 | 0.01 | 301 | 110. | 372. | 24. | | 38. | * | | * | |
| 225 | 14. | -70. | 22. | | 15. | * | | * | 302 | 110. | -15. | 27. | * | | * | | * | |
| 226 | 14. | 219. | 72. | | 54. | * | | * | 303 | 111. | -6. | 45. | | 22. | * | | * | |
| 227 | 16. | 17. | 335. | | 37. | * | | * | 304 | 112. | -195. | 48. | | 45. | * | | * | |
| 228 | 18. | 30. | 203. | | 37. | * | | * | 305 | 113. | -212. | 8. | * | | * | | * | |
| 229 | 20. | -109. | 266. | | 29. | * | | * | 306 | 114. | 321. | 9. | * | | * | | * | |
| 230 | 20. | -36. | 188. | | 41. | * | | * | 307 | 115. | 228. | 23. | | 27. | * | | * | |
| 231 | 24. | -141. | 54. | | 32. | * | | * | 308 | 117. | -82. | 76. | | 36. | * | | * | |
| 232 | 24. | 12. | 157. | | 32. | * | | * | 309 | 124. | -22. | 317. | | 48. | * | | * | |
| 233 | 25. | 25. | 45. | | 15. | * | | * | 310 | 124. | -112. | 80. | | 54. | * | | * | |
| 234 | 26. | -9. | 238. | | 56. | | 0.54 | -0.01 | 311 | 125. | 28. | 60. | | 32. | * | | * | |
| 235 | 27. | 125. | 24. | | 15. | | 0.54 | -0.01 | 312 | 125. | -186. | 145. | | 39. | * | | * | |
| 236 | 27. | -16. | 454. | | 52. | * | | * | 313 | 126. | -121. | 89. | | 44. | * | | * | |
| 237 | 27. | -153. | 25. | | 18. | * | | * | 314 | 127. | -171. | 143. | | 57. | * | | * | |
| 238 | 27. | 357. | 13. | | 13. | * | | * | 315 | 130. | -85. | 201. | | 31. | * | | * | |
| 239 | 29. | -130. | 62. | | 12. | * | | * | 316 | 131. | -6. | 29. | * | | * | 0.79 | | -0.30 |
| 240 | 32. | -45. | 28. | * | | * | | * | 317 | 131. | -131. | 160. | | 28. | * | | * | |
| 241 | 33. | -194. | 15. | | 26. | * | | * | 318 | 131. | 88. | 95. | | 64. | * | | * | |
| 242 | 33. | -6. | 62. | | 17. | * | | * | 319 | 132. | -244. | 59. | | 42. | * | | * | |
| 243 | 35. | -113. | 485. | | 63. | | 1.09 | 0.06 | 320 | 134. | -124. | 1286. | | 109. | * | | * | |
| 244 | 36. | -213. | 18. | | 24. | * | | * | 321 | 135. | -134. | 292. | | 33. | | 0.79 | | -0.30 |
| 245 | 36. | 74. | 89. | | 42. | * | | * | 322 | 140. | 12. | 40. | | 26. | * | | * | |
| 246 | 36. | 230. | 206. | | 60. | * | | * | 323 | 141. | -32. | 166. | | 38. | | 0.63 | | -0.41 |
| 247 | 36. | 11. | 256. | | 61. | * | | * | 324 | 144. | 58. | 14. | | 12. | * | | * | |
| 248 | 37. | -36. | 33. | | | * | | * | 325 | 146. | 24. | 29. | | 25. | * | | * | |
| 249 | 39. | -198. | 26. | | 37. | * | | * | 326 | 147. | -68. | 17. | * | | * | | * | |
| 250 | 39. | 221. | 20. | | 27. | * | | * | 327 | 148. | 7. | 137. | | 23. | * | | * | |
| 251 | 41. | 139. | 34. | | 29. | * | | * | 328 | 149. | -241. | 65. | | 29. | * | | * | |
| 252 | 41. | -59. | 246. | | 82. | * | | * | 329 | 154. | -84. | 17. | | 12. | * | | * | |
| 253 | 44. | -253. | 11. | * | | * | | * | 330 | 157. | -239. | 1579. | | 62. | * | | * | |
| 254 | 45. | -24. | 24. | * | | * | | * | 331 | 160. | -244. | 172. | | 21. | * | | * | |
| 255 | 46. | -262. | 26. | | 23. | * | | * | 332 | 160. | 147. | 29. | | 32. | * | | * | |
| 256 | 47. | 82. | 4940. | | 52. | * | | 0.09 | 333 | 160. | -42. | 18. | | 33. | * | | * | |
| 257 | 48. | 304. | 67. | | 36. | * | | * | 334 | 162. | 142. | 17. | | 10. | * | | * | |
| 258 | 50. | 232. | 22. | | 9. | * | | * | 335 | 162. | -239. | 340. | | 37. | * | | * | |
| 259 | 51. | -122. | 107. | | 34. | * | | * | 336 | 163. | -177. | 42. | | 47. | * | | * | |
| 260 | 51. | -209. | 8. | * | | * | | * | 337 | 163. | -119. | 179. | | 23. | * | | * | |
| 261 | 51. | -14. | 105. | | 35. | * | | * | 338 | 166. | -37. | 36. | | 40. | * | | * | |
| 262 | 53. | 77. | 63. | * | | * | | * | 339 | 168. | -134. | 145. | | 44. | * | | * | |
| 263 | 53. | 30. | 107. | | 24. | | 0.36 | 0.06 | 340 | 168. | 149. | 1786. | | 2. | | 0.98 | | 0.21 |
| 264 | 53. | -193. | 139. | | 32. | * | | * | 341 | 169. | -162. | 140. | | 50. | * | | * | |
| 265 | 54. | -161. | 8. | * | | * | | * | 342 | 170. | -243. | 1110. | | 27. | * | | * | |
| 266 | 56. | -100. | 6. | * | | * | | * | 343 | 171. | -146. | 30. | | 21. | * | | * | |
| 267 | 56. | 88. | 100. | | 32. | * | | * | 344 | 174. | -143. | 13. | * | | * | | * | |
| 268 | 57. | -54. | 938. | | 85. | | 0.65 | 0.00 | 345 | 176. | -133. | 3049. | | 63. | * | | * | |
| 269 | 57. | -44. | 16. | * | | * | | * | 346 | 176. | -88. | 17. | | 2. | * | | * | |
| 270 | 58. | 76. | 34. | | 7. | * | | * | 347 | 176. | -21. | 651. | | 33. | * | | * | |
| 271 | 63. | 29. | 274. | | 69. | * | | * | 348 | 178. | 127. | 64. | | 52. | * | | * | |
| 272 | 63. | -54. | 1010. | | 107. | | 0.65 | 0.00 | 349 | 180. | -20. | 554. | | 20. | * | | * | |
| 273 | 65. | 84. | 13. | | 10. | * | | * | 350 | 184. | -23. | 396. | | 32. | * | | * | |
| 274 | 65. | -93. | 38. | | 17. | * | | * | 351 | 187. | -201. | 249. | | 28. | * | | * | |
| 275 | 66. | -38. | 547. | | 46. | * | | * | 352 | 189. | -176. | 33. | | 22. | * | | * | |
| 276 | 67. | 75. | 28. | | 30. | * | | * | 353 | 192. | 115. | 17. | | 25. | * | | * | |
| 277 | 70. | 90. | 139. | | 72. | * | | * | 354 | 193. | -218. | 43. | | 33. | * | | * | |
| 278 | 71. | 83. | 9. | * | | * | | * | 355 | 194. | -325. | 39. | | 34. | * | | * | |
| 279 | 76. | -2. | 77. | | 33. | * | | * | 356 | 195. | -330. | 34. | | 21. | * | | * | |
| 280 | 77. | 248. | 94. | * | | * | | * | 357 | 195. | -175. | 146. | | 77. | * | | * | |
| 281 | 79. | -255. | 46. | | 67. | * | | * | 358 | 198. | 118. | 59. | | 52. | * | | * | |
| 282 | 80. | 77. | 452. | | 90. | * | | * | 359 | 204. | -15. | 68. | | 42. | * | | * | |
| 283 | 81. | -16. | 20. | * | | * | | * | 360 | 208. | -218. | 18. | | 25. | * | | * | |
| 284 | 83. | 284. | 32. | | 35. | * | | * | 361 | 211. | -207. | 21. | | 23. | * | | * | |
| 285 | 84. | 17. | 173. | | 28. | * | | * | 362 | 219. | -223. | 18. | | 24. | * | | * | |
| 286 | 84. | -106. | 15. | | 27. | * | | * | 363 | 222. | -324. | 25. | | 23. | * | | * | |
| 287 | 88. | 47. | 46. | | 23. | * | | * | 364 | 223. | 92. | 75. | | 40. | * | | * | |
| 288 | 91. | -131. | 31. | | 38. | * | | * | 365 | 281. | -135. | 35. | | 24. | * | | * | |
| 289 | 93. | 2. | 94. | | 34. | * | | * | 366 | 301. | -1. | 53. | | 72. | * | | * | |
| 290 | 94. | -104. | 125. | | 56. | | 0.53 | -0.14 | 367 | 304. | 45. | 39. | | 57. | * | | * | |
| 291 | 97. | -10. | 159. | | 32. | | 0.69 | -0.25 | 368 | 312. | 17. | 55. | | 44. | * | | * | |
| 292 | 101. | -223. | 124. | | 87. | * | | * | 369 | 326. | -64. | 20. | | 34. | * | | * | |

**Table 2.** Line intensity ratios in the diffuse background

| X (arc sec) | Y (arc sec) | log H/N | log N/S |
|---|---|---|---|
| 1. | 23. | 0.55 | -0.27 |
| 45. | -35. | 0.41 | -0.29 |
| 72. | -70. | 0.33 | -0.01 |
| 84. | -87. | 0.45 | -0.21 |
| -59. | 43. | 0.84 | -0.41 |
| -37. | 25. | 0.61 | -0.34 |
| -132. | 136. | 0.43 | -0.41 |

Table 2 concerns spectrophotometric data obtained for 7 directions in the diffuse medium:

- *Columns 1 and 2* give the $X, Y$ offset coordinates of the observed directions;
- *Columns 3 and 4* list respectively the logarithmic line intensity ratios $I(H\alpha)/I([NII])$ and $I([NII])/I([SII])$, as defined hereabove.

## 5. Discussion

### 5.1. Distribution of Diameters

Figure 5a shows the histogram of *effective diameters* in 1′ bins for 303 regions. The shape of the distribution is similar to that commonly observed in other galaxies with a truncation towards

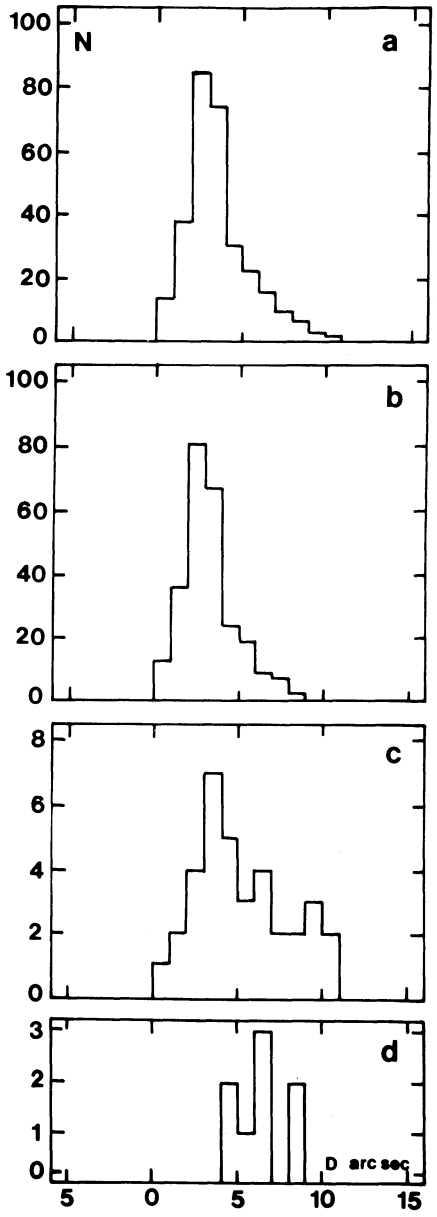


**Fig. 5.** Histograms of *effective diameters* in bins of 1″; **a:** for all the resolved HII regions in NGC 2403; for regions with flux $F$ in units of $10^{-16}$ erg cm$^{-2}$ s$^{-1}$, **b:** $F < 879$, **c:** $879 < F < 2572$, and **d:** $F > 2572$.

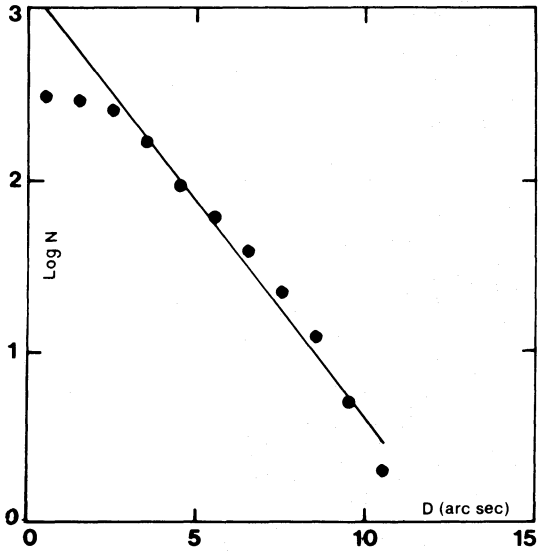


**Fig. 6.** Frequency distribution of HII region diameters in NGC 2403. The number of regions $N$ with diameter larger than $D$ (arcsec) is plotted as a function of log $D$. The line is the best fitting exponential law, when neglecting the point corresponding to the smallest diameters for which the statistic is limited by instrumental effect.

the small diameters. As previously discussed (Sivan, 1977; Hodge, 1976; Milliard and Marcelin, 1981) this typical shape probably results from an observational limit in angular resolution. Figures 5b-d display the same histogram but respectively for low, medium and high luminosity nebulae: the distributions in these figures are similar to those obtained for other galaxies e.g. for M 81 (Petit et al., 1988). The low-luminosity distribution (Fig. 5b.) is about the same as the general distribution shown in Fig. 5a; this is not surprising since 86% of the regions for which we have measured a diameter lie in the low-intensity range. On the contrary, the brightest regions (Fig. 5d) show an almost flat distribution. For regions of intermediate intensity, the diameter distribution (Fig. 5c) resembles that in Figs. 5a and 5b but with a peak shifted towards the large diameters and then an abrubt decrease. Five regions have diameters larger than 9″ and two regions have diameters between 10 and 11″. If we assume for NGC 2403 a distance $d = 2.6$ Mpc (de Vaucouleurs, 1978), the five largest regions have linear diameters of 125 – 140 pc. The largest diameters would be in the range 160 – 175 pc assuming $d = 3.3$ Mpc (Sandage and Tammann, 1968).

In Fig. 6 we have plotted in a logarithmic scale the number of regions $N$ with diameter larger than $D$ as a function of the diameter $D$ in arc sec. It appears that the frequency distribution of diameters in NGC 2403 follows the law found by van den Bergh (1981), i.e.:

$$N = N_\circ \exp(-D/D_\circ),$$

with $N_\circ = 1346$ and $D_\circ = 1''.72$. Depending on the assumed distance to the galaxy, we have $D_\circ = 22$ pc ($d = 2.6$ Mpc) or $D_\circ = 27$ pc ($d = 3.3$ Mpc).

Due to a rather short equivalent focal length of our instrument, it appears difficult to resolve unambiguously narrow filamentary structures at the distance of NGC 2403. This can explain why bubble-like HII regions (or *HII rings*) do not look as prominent in Fig. 1a as they do in similar images of M 33 obtained in identical conditions (Courtès et al. 1987). However, in the high-resolution photograph of the central part of the galaxy published by Lynds (1974) and reprinted in totality by Fierro et al. (1986), several bubble-like HII features conspicuously appear, especially around the brightest HII complexes. These HII rings correspond to our regions #98, #176 + #187, to the southern extension of our region #44 (including regions #58 and #60) and to the northern extension of region #298. Since we did not feel safe to select an unbiased sample of these features among the regions in our catalogue, we did not try to derive a characteristic diameter value of the HII bubbles of NGC 2403.

### 5.2. *Luminosity function*

Table 3 gives the luminosity function for the 366 measured HII regions. The first flux bin contains an almost certainly incomplete sample due to a variable detection threshold. (The

**Table 3.** Distribution of luminosities

| FLUX BIN[a] | $N_{obs}$ [b] | $N_{ave}$ [c] |
|---|---|---|
| 0000 - 00039 | 135 | 135 |
| 0039 - 00078 | 078 | 078 |
| 0078 - 00117 | 028 | 028 |
| 0117 - 00156 | 025 | 025 |
| 0156 - 00195 | 017 | 017 |
| 0195 - 00273 | 020 | 010 |
| 0273 - 00390 | 019 | 006.33 |
| 0390 - 00585 | 020 | 004.00 |
| 0585 - 01950 | 016 | 000.46 |
| 1950 - 31200 | 008 | 000.01 |

Notes to Table 3:
a: fluxes are in units of $10^{-16}$ erg cm$^{-2}$ s$^{-1}$
b: observed number of regions per bin
c: averaged number per bin of $39 \times 10^{-16}$ erg cm$^{-2}$ s$^{-1}$

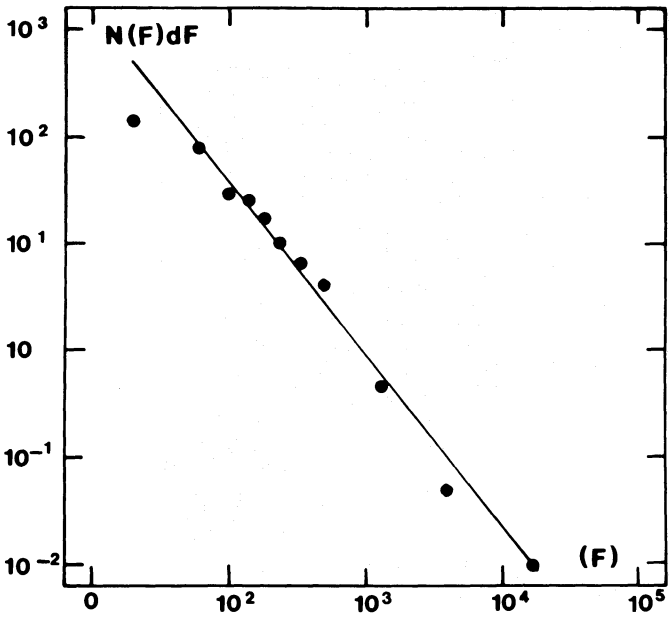


**Fig. 7.** Luminosity function of the 366 HII regions detected in NGC 2403. The number of regions $N$ in bins of 39 $10^{-16}$ erg cm$^{-2}$ s$^{-1}$ is plotted as a function of the flux in units of $10^{-16}$ erg cm$^{-2}$ s$^{-1}$, according to Table 3. The straight line is the best power law fit when neglecting the point at the very faint end where the sampling is incomplete.

detection of the faintest nebulae depends on the background noise and on the background level. This level is not constant over the galaxy because of diffuse emission in the arms). For large fluxes the statistic is very poor and we have computed mean values averaged over several adjacent bins, as usually done (e.g. Kennicutt and Hodge, 1980; Comte and Duquennoy, 1982). Figure 7 displays the luminosity function in the (log $N$, log $F$)-plane. If one excludes the point at the very faint end where sampling is incomplete, it appears that the function is

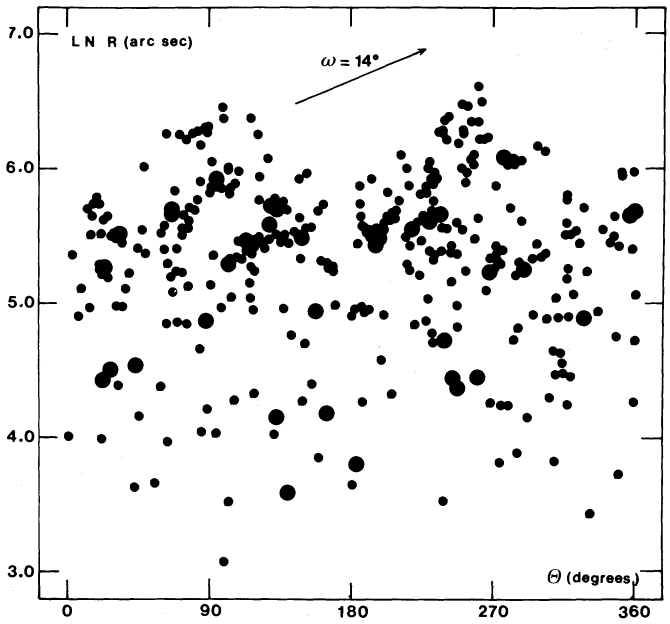


**Fig. 8.** A plot of the neperian logarithm of the galactocentric distance $R$ versus position angle $\Theta$, for the HII regions detected in NGC 2403 ($\Theta$ and $R$ are both deprojected in the plane of the galaxy). The arrow indicates the slope of the representation of a logarithmic spiral arc with a pitch angle of 14°. Large dots are for HII regions with Hα flux larger than $5 \times 10^{-14}$ erg cm$^{-2}$ s$^{-1}$ (small dots for other regions).

closely approximated by a power law (as is generally the case for spiral galaxies)

$$N(F) = k F^{-\alpha},$$

where $\alpha = 1.60$ and $k = 10^{4.8}$ with $F$ in units of $10^{-16}$ erg cm$^{-2}$ s$^{-1}$. It should be noted that we have also calculated a (cumulative) *integral luminosity function* for NGC 2403 in the way used by Kennicutt et al. (1989): it compares quite well with that obtained by these authors.

### *5.3. Spatial distribution of the HII regions across the disk: the elusive spiral structure*

Danver (1942) claimed that he succeeded to fit the spiral structure of NGC 2403, as observed in blue light, with two logarithmic arms of respective pitch angles 15.1 and 13.4° (using $P.A. = 125°$ and $i = 54°.5$ as deprojection parameters). The quality of this fit (estimated from an *agreement parameter* of 0.04 and 0.09 for the two arms respectively) was considered as quite fair (with repect, for instance, to M 33). If we plot the deprojected HII regions distribution in the plane ($\Theta$, $\ln r$) (using $P.A. = 125°$ and $i = 60°$ as recommended by Wevers, 1984), $\Theta$ and $r$ being the polar coordinates in the plane of the galaxy, clear logarithmic spiral features would appear as accumulation of points along linear segments. However, Figure 8 shows a very confused diagram, in which there appears no conspicuous regular spiral pattern. The situation does not improve very much if we segregate the HII regions according to their fluxes, since it could be advocated that fainter regions may form indistinctely both along arms and in the interarm (Rumstay and Kaufmann, 1983). In Fig. 8, the slope of a segment corresponding to a theoretical logarithmic spiral arm of pitch angle 14° is indicated. This result is in good agreement

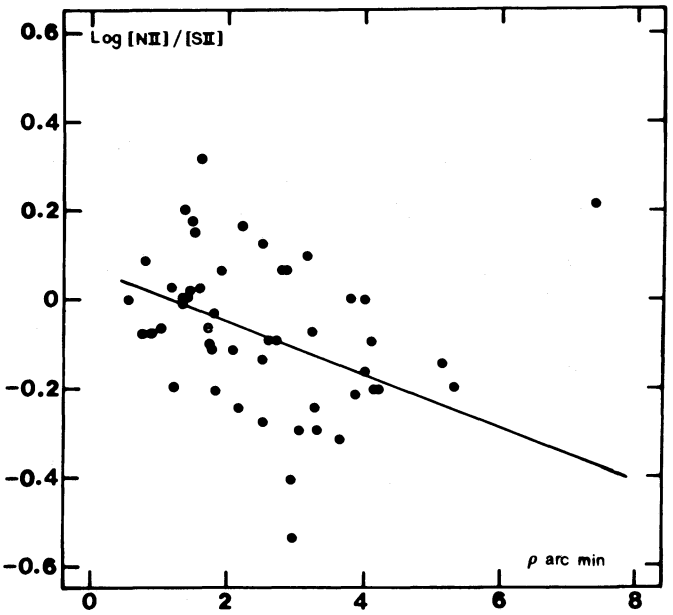


**Fig. 9.** A plot of the $[NII]/[SII]$ ratio versus galactocentric distance (in the plane of the galaxy) for 50 HII regions. The slope of the regression line indicates an $N^+/S^+$ abundance gradient of $-0.078 \pm 0.024$ kpc$^{-1}$, assuming a distance of 2.6 Mpc and neglecting the point at the right end of the diagram.

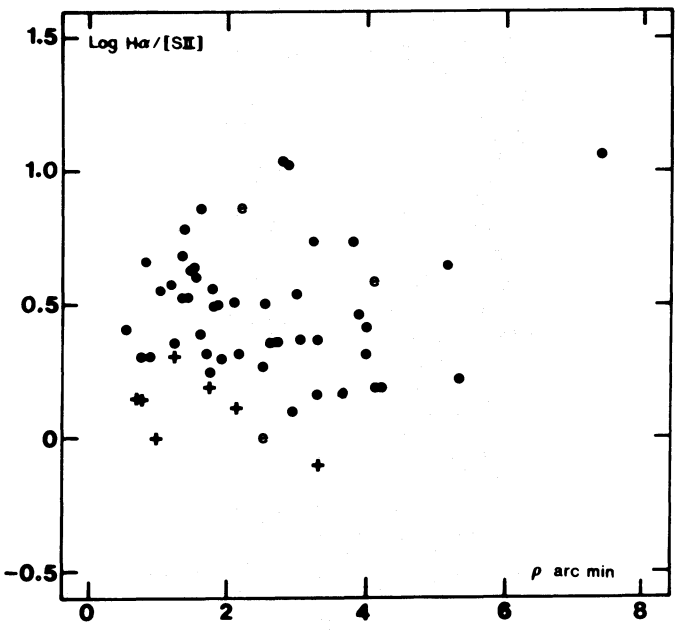


**Fig. 10.** A plot of the $H\alpha/[SII]$ ratio versus galactocentric distance (in the plane of the galaxy) for *classical* HII regions (dots) and for regions of diffuse ionized background (crosses). The last regions are systematically found lower than the former ones: this indicates differences in excitation conditions.

with that of Hodge and Kennicutt (1983b): their rectified face-on map of the HII regions in NGC 2403 does not show any spiral pattern.

Since a photograph of NGC 2403 taken in blue light quite clearly shows a spiral pattern (see e.g. Plate 9 in Sandage and Bedke, 1988), we must invoke a large width of the locus of massive star formation across the spiral arms to explain the loss of contrast in Fig. 8. This may be related to the luminosity class III of the galaxy, corresponding to the absence of *grand design*, this in turn being probably related to an absence or a weakness of shock wave along the spiral front. A similar situation is examplified in NGC 300 of same type and luminosity class: the Hα photograph of this galaxy practically does not exhibit any spiral distribution (see Fig. 1a in Deharveng et al., 1988).

We remain aware that a Fourier analysis of the HII regions distribution, which can take into account the angular extent of the spiral features, would probably enable to recover the spiral structure and set a quantitative evaluation of the *width* of the spiral arms (Considere and Athanassoula, 1982) but this is beyond the scope of the present paper.

### 5.4. *N/S abundance gradient*

Determining chemical abundances in the HII regions of NGC 2403 would have required the observation of a larger number of emission lines. However, Fierro et al. (1986) have shown – in particular for NGC 2403 – that most of the $I([NII])/I([SII])$ line ratio gradient could be due to an abundance gradient, i.e. that under certain assumptions

$$I([NII])/I([SII]) \simeq N^+/S^+.$$

In these conditions, they find in the plane of NGC 2403 a logarithmic $N^+/S^+$ gradient of $-0.074 \pm 0.034$ kpc$^{-1}$. Combining their observations with those by Smith (1975) and McCall et al. (1985), they find a gradient of $-0.073 \pm 0.023$ kpc$^{-1}$, assuming $d = 2.6$ Mpc. In Fig. 9 we have plotted the $I([NII])/I([SII])$ ratios listed in Table 1 as a function of galactocentric distance (in the plane of the galaxy). The gradient is found to be $-0.078 \pm 0.024$ kpc$^{-1}$, assuming the same distance to the galaxy, $P.A. = 125°$ and $i = 60°$. It is interesting to note that we find practically the same value as Fierro et al. (1986). The basic difference between the two studies is that we observed the $[NII]/[SII]$ ratio on 50 HII regions including faint ones, while Fierro et al. calculated their gradient on the basis of only 9 bright regions.

### 5.5. *Excitation in the diffuse ionized medium*

Figure 10 is a plot of the $H\alpha/[SII]\lambda 6717 + 6731$ line intensity ratio against galactocentric distance for the *classical* HII regions (Table 1) and for regions of diffuse ionized background (Table 2). At a given galactic radius, the $H\alpha/[SII]$ ratio is found to be significantly smaller in the diffuse background than in the HII regions. This can be related to a result obtained in our Milky Way and, we think, interpreted in similar terms: either an extremely dilute ionizing radiation field (Mathis, 1986; Reynolds, 1988) or a combination of photoionization and weak shocks (Sivan et al., 1986; Brand and Mathis, 1978) might account for the excess of brightness of the [SII] doublet when observed in the diffuse ionized medium, outside the *classical* well defined HII regions of the galactic arms.

### 5.6. *Radial behaviour of massive star formation*

For all what follows, the distance to NGC 2403 is assumed to be 3.3 Mpc. The Hα flux data in Table 1 have been integrated over annuli of constant step 1′ (= 960 pc) in radius. Figure 11a shows

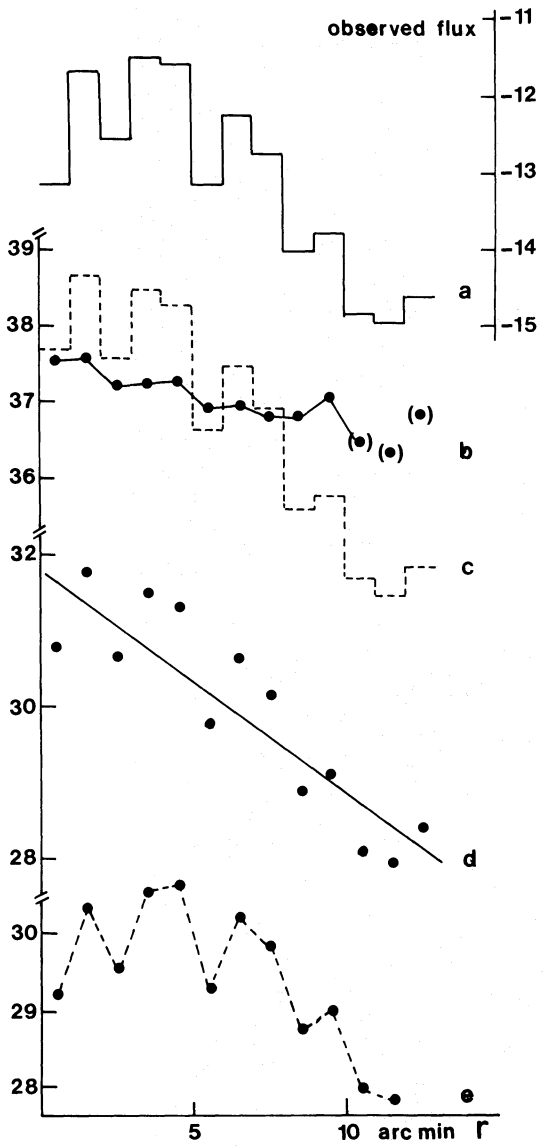


**Fig. 11.** Radial trends of massive star formation tracer. **a** *(continuous line)*: logarithm of the total observed Hα flux per annulus of 1′ wide (in erg $cm^{-2}s^{-1}$), **b** *(dots)*: median value of the intrinsic logarithmic Hα flux (in erg $s^{-1}$) per HII region per annulus, corrected for extinction (see text), **c** *(dotted line)*: logarithm of the total intrinsic Hα flux per annulus per unit area of disk (in erg $s^{-1}kpc^{-2}$), **d** *(dots)*: same as **c** but normalized to the surface density of neutral hydrogen (in erg $s^{-1}M_{\odot}^{-1}$), **e** *dotted line*: logarithmic ratio of the Hα total intrinsic flux to the corrected projected near-uv luminosity (in erg $s^{-1}L_{\odot}(U')^{-1}$).

the resultant total observed flux distribution, which rises until 4–5′ from the center and declines quickly outwards. However, to use an HII region radial flux distribution as a tracer of a massive star formation radial gradient, i) it is necessary to normalize the crude observed distribution to the projected area, ii) it seems better to use intrinsic fluxes (emitted) rather than observed ones: here sets up the problem of extinction corrections. The observed fluxes were therefore transformed into intrinsic fluxes through the following procedure:

- A Galactic line-of-sight color excess $E(B-V) = 0.04$ mag, adopted from Burstein and Heiles (1984) leads to a Galactic extinction correction of 0.10 mag at Hα following the standard Savage-Mathis extinction law.
- From the spectrophotometry of 6 bright regions by McCall et al. (1985), and 3 others by Fierro et al. (1986), we derive an average extinction, internal to NGC 2403, of 0.45 mag at Hα. If we assume that the absorbing matter is not mixed with the ionized gas, we get a total average extinction correction of 0.55 mag at Hα and hence a logarithmic correction of the fluxes of 0.22. We stress that this oversimplified view i) does not take into account a probable gradient in dust content across the disk of the galaxy, extinction being probably higher in the central regions (but the spectrophotometric data are by far too scanty), ii) probably underestimates the internal extinction as it is known from several comparisons between Balmer decrement-derived extinctions and thermal radio continuum HII fluxes (see e.g. Israel and Kennicutt, 1980).

The total integrated intrinsic Hα flux emitted by the resolved HII regions of NGC 2403 is 1.9 $10^{40}$ erg $s^{-1}$ with the adopted corrections. If we use an average internal extinction of 1.1 mag at Hα we find 3.4 $10^{40}$ erg $s^{-1}$ . The same computation applied to the total observed Hα flux of the HII regions in NGC 300, from the data by Deharveng et al. (1988), yields, at 1.66 Mpc, a total intrinsic flux of 1.3 $10^{40}$ erg $s^{-1}$. In the sample of disk galaxies studied by Kennicutt (1983), there are 17 objects classified Sc III in Sandage and Tammann (1981); the mean value of the emitted flux for these galaxies is 2.4 $10^{41}$ erg $s^{-1}$ with that extinction correction; using a Hubble constant of 75 km $s^{-1}$ $Mpc^{-1}$ instead of 50, as used by Kennicutt, leaves a discrepancy of more than a factor of three. We are led to conclude that:

i) either the intrinsic fluxes in Kennicutt's paper are overestimated by the propagation of some systematic calibration error, or our fluxes and those of Deharveng et al. as well are underestimated ;
ii) or NGC 2403 and NGC 300 are both exceptionally quiet objects with respect to star formation;
iii) or a very substantial part of the total Hα flux is present as diffuse light in the observed image and not recovered when selecting only the resolved regions: this would be in contradiction with the finding by Kennicutt and Hodge (1980) that in NGC 628 (Sc I) 80% of the total Hα flux is contributed by discrete HII regions, but unpublished CCD data obtained by Hodge (private communication) show that the diffuse Hα light in NGC 2403 looks quite a bit brighter than that in NGC 628.

The median value of the Hα flux per annulus was also computed from the histogram of the observed fluxes in each annulus. This quantity is shown in Fig. 11b; although the statistics becomes poor beyond $r = 9'$, a slow decrease with increasing $r$ can be inferred; within 10 kpc, the median Hα flux decreases by a factor of 6. If we consider that this median value is representative of the *typical* ionizing power of a newborne cluster populated with massive stars, it means that the efficiency of the formation of these massive stars has declined in the same proportion, or, in other words, that the luminosity function of these massive stars has been scaled down along the same factor.

The *rate* of massive star formation is better represented through the ratio of the corrected Hα intrinsic fluxes to the available reservoir, that is, the projected mean surface density of neutral hydrogen. This latter quantity is given by Wevers (1984) and the radial run of the ratio is shown in Fig. 11c. The radial decrease of the ratio is very regular and can be fitted with a

**Table 4.** Massive star formation tracers

| Annulus | log observed Hα flux (erg cm$^{-2}$ s$^{-1}$) | log intrinsic Hα flux (erg s$^{-1}$ kpc$^{-2}$) | log median intrinsic Hα flux (erg s$^{-1}$) | log f ($\mathrm{erg\ s^{-1}\ M_\odot^{-1}}$) | log g ($\mathrm{erg\ s^{-1}\ L_\odot(U')^{-1}}$) |
|---|---|---|---|---|---|
| 0′- 1′ | -13.15 | 37.68 | 37.53 | 30.77 | 29.19 |
| 1′- 2′ | -11.70 | 38.66 | 37.57 | 31.75 | 30.37 |
| 2′- 3′ | -12.57 | 37.57 | 37.20 | 30.65 | 29.50 |
| 3′- 4′ | -11.52 | 38.47 | 37.26 | 31.50 | 30.56 |
| 4′- 5′ | -11.61 | 38.27 | 37.28 | 31.31 | 30.63 |
| 5′- 6′ | -13.17 | 36.63 | 36.90 | 29.75 | 29.24 |
| 6′- 7′ | -12.26 | 37.46 | 36.96 | 30.65 | 30.22 |
| 7′- 8′ | -12.75 | 36.91 | 36.82 | 30.15 | 29.82 |
| 8′- 9′ | -14.02 | 35.59 | 36.78 | 28.87 | 28.74 |
| 9′-10′ | -13.79 | 35.77 | 37.08 | 29.10 | 29.02 |
| 10′-11′ | -14.85 | 34.67 | (36.48) | 28.07 | 27.99 |
| 11′-12′ | -15.04 | 34.44 | (36.33) | 27.91 | 27.86 |
| 12′-13′ | -14.62 | 34.82 | (36.84) | 28.39 | - |

linear regression: this implies that the total Hα flux per solar mass of HI declines exponentially; the e-folding length indicated by the fit in Fig. 11d is 1.4 kpc, slightly shorter than the length scale of the disk luminosity distribution in the visible [1.6 kpc from Okamura et al. (1977) and 2 kpc from Wevers (1984)] and than the length scale of the radial distribution of HII regions (2.0 kpc) found by Hodge and Kennicutt (1983b).

Finally, it is interesting to compare the Hα flux to another tracer of young star formation: the near-ultraviolet U band luminosity. This quantity is also available from Wevers (1984), who used an U' photometric band tied to the UBV system through the relation:

$$U' = 1.08\,U - 0.08\,B + 0.24\,(B-V).$$

Applying this to the Sun, with $B_\odot = 5.48$, $(B-V)_\odot = 0.64$ and $U_\odot = 5.61$, we get an absolute solar magnitude $U'_\odot = 5.77$ and the U' projected luminosity in $L(U')_\odot$ pc$^{-2}$, follows from the U' surface brightness:

$$L_{U'} = 10^{0.4[21.57+5.77-m_{U'}(0)]},$$

where $m_{U'}(0)$ is the surface brightness in magnitude, corrected for extinction and inclination. We assume here a Galactic foreground extinction of $A_{U'} = 5E(B-V) = 0.20$ mag; the highly uncertain internal extinction is not taken into account.

$$m_{U'}(0) = m_{U'} - 0.20 - 2.5\log(\cos i) = m_{U'} + 0.55$$

Table 4 summarizes all the relevant information on the massive star formation tracers as follows:

- *Column 1*: annulus in the plane of the galaxy
- *Column 2*: log of total observed Hα flux in erg cm$^{-2}$ s$^{-1}$
- *Column 3*: log of total intrinsic Hα corrected flux, per unit surface, in erg s$^{-1}$ kpc$^{-2}$
- *Column 4*: log of the median Hα intrinsic flux, in erg s$^{-1}$
- *Column 5*: log of the ratio f of the Hα intrinsic flux to the surface density of neutral gas, in erg s$^{-1}$ $M_\odot^{-1}$
- *Column 6*: log of the ratio g of the Hα intrinsic flux to the corrected U' projected luminosity, in erg s$^{-1}L_\odot(U')^{-1}$

Figure 11e shows the trend of g with radius: g appears reasonably constant between 0 and 8′ from the center (where the surface density of HI drops below 5 $M_\odot$ pc$^{-2}$) and decreases abruptly outwards. Even when taking into account possible large errors in the U' surface photometry at the outer edge of NGC 2403, this sudden decrease seems real, as Wevers (1984) noticed an important negative color gradient in (U'-F) color (closely matching the more familiar (U-R) color). The U' spectral band, with its effective wavelength centered near 3750 Å, should be a good tracer of the extreme Population I but not only of the fraction exclusively containing the ionizing stars: late O and early B stars would contribute a lot to the flux observed in U', but these stars do not produce sufficient Lyman continuum flux to make HII regions powerful enough to be seen as extended Hα sources at 3.3 Mpc. Looking at the disk of NGC 2403 beyond 9′ (= 8.6 kpc) from the center, we are therefore led to admit that the galaxy becomes gradually unable to form very massive stars: the Initial Mass Function should be truncated there at a lower mass cutoff than in the central regions; this in turn may be due to a decrease in the local average density of gas available for star formation.

## 6. Conclusion

From Hα narrow-band photographs, we have identified 366 HII regions in the spiral galaxy NGC 2403. A catalogue lists for the identified regions $X,Y$ offset positions, Hα fluxes and angular diameters. Also, for 52 regions, it gives the $H\alpha/[NII]$ and $[NII]/[SII]$ line intensity ratios. These ratios have also been measured in several directions of the diffuse ionized background. The main results we have derived from these data can be summarized as follows:

- the frequency distribution of the HII region diameters follows van den Bergh's law;
- the Hα luminosity function is well represented by a power-law;
- the $N^+/S^+$ abundance gradient is found to be in agreement with previous determinations based on fewer and brighter regions;
- the [SII]$\lambda\lambda$6717,6731 Å lines are found significantly brighter in the diffuse background than in the *classical* HII regions, probably indicating differences in excitation conditions;
- the spatial distribution of the HII regions in the plane of the galaxy does *not* reveal any conspicuous spiral structure;

- the rate of massive star formation regularly decreases from the center to the outer regions of NGC 2403, but it is suggested that beyond about 9′ from the center the Initial Mass Function is truncated at a lower mass cutoff than in the central regions.

*Acknowledgements*. The Hα observations reported in this paper are part of a survey of nearby galaxies carried out at the Special Astrophysical Observatory (SAO) owing to an agreement between the USSR Academy of Sciences and the french Ministère des Relations Extérieures. Both these organizations are acknowledged. It is a pleasure to thank the Director and all the scientific and technical staff of the SAO – in particular Dr. S. Dodonov –, whose help was greatly appreciated. Special thanks are due to G. Courtès who initiated the program and contributed greatly to its success, J. Lequeux for kindly providing us with a Grism plate of NGC 2403 and M. Petit for her help during the observations. Some data presented in this paper were collected at the Observatoire de Haute Provence du CNRS whose Director and technical staff are acknowledged. Data reduction and final presentation of the results benefitted by the help of B. Debray, C. Chisholm, R. Donas, P. Figon, J.-P. Goudal, L. Leporati and J. Martinis: they are greatly acknowledged.

## References

Bonnarel, F., Boulesteix, J., Marcelin, M.: 1986, *Astron. Astrophys. Suppl. Ser* **66**, 149
Comte, G., Duquennoy, A.: 1982, *Astron. Astrophys.* **114**, 7
Comte, G., Monnet, G.: 1974, *Astron. Astrophys.* **33**, 161
Considere, S., Athanassoula, E.: 1982, *Astron. Astrophys.* **111**, 28
Courtès, G., Petit, H., Sivan, J.-P., Dodonov., S., Petit, M.: 1987, *Astron. Astrophys.* **174**, 28
Danver, C.-G.: 1942, *Annals Lund Obs. N°* 10
Deharveng, J.-M., Pellet, A.: 1970, *Astron. Astrophys.* **9**, 181
Deharveng, L., Caplan, J., Lequeux, J., Azzopardi, M., Breysacher, J., Tarenghi, M., Westerlund, B.: 1988, *Astron. Astrophys. Suppl. Ser.* **73**, 407
de Vaucouleurs, G.: 1978, *Astrophys. J.* **224**, 14
de Vaucouleurs, G., de Vaucouleurs, A., Corwin, H.G.: 1976, *Second Reference Catalogue of Bright Galaxies*, Univ. of Texas Press, Austin
Fierro, J., Torres-Peimbert, S., Peimbert, M.: 1986, *Publ. Astron. Soc. Pac.* **98**, 1032
Hodge, P.W.: 1969, *Astrophys. J. Suppl. Ser.* **18**, 73
Hodge, P.W.: 1976, *Astrophys. J.* **205**, 728
Hodge, P.W., Kennicutt, R.C.: 1983a, *Astron. J.* **88**, 296
Hodge, P.W., Kennicutt, R.C.: 1983b, *Astrophys. J.* **267**, 563
Israel, F.P., Kennicutt, R.C.: 1980, *Astrophysical Letters* **21**, 1
Jensen, E.B., Strom, K.M., Strom, S.E.: 1976, *Astrophys. J.* **209**, 748
Kennicutt, R.C.: 1979, *Astrophys. J.* **228**, 394
Kennicutt, R.C.: 1983, *Astrophys. J.* **272**, 54
Kennicutt, R.C., Hodge, P.W.: 1980, *Astrophys. J.* **241**, 573
Kennicutt, R.C., Edgar, B.K., Hodge, P.W.: 1989, *Astrophys. J.* **337**, 761
Lynds, B.T.: 1974, *Astrophys. J. Suppl. Ser.* **28**, 391
McCall, M.L.: 1982, *University of Texas Publ. in Astronomy N°* 20
McCall, M.L., Rybski, P.M., Shields, G.A.: 1985, *Astrophys. J. Suppl. Ser.* **57**, 1
Milliard, B., Marcelin, M.: 1981, *Astron. Astrophys.* **95**, 59
Okamura, S., Takase, B., Kodaira, K.: 1977, *Publ. Astr. Soc. Japan* **29**, 567
Petit, H., Sivan, J.-P., Karachentsev, I.D.: 1988, *Astron. Astrophys. Suppl. Ser.* **74**, 475
Reynolds, R.J.: 1988, *Astrophys. J.* **333**, 341
Reynolds, R.J.: 1989, *IAU Symposium N° 139*, Eds.Bowyer and Leinert
Rumstay, K.S., Kaufman, M.: 1983, *Astrophys. J.* **274**, 611
Sandage, A., Bedke, J.: 1988, *Atlas of Galaxies useful for measuring the cosmological distance scale*, NASA, Washington
Sandage, A., Tammann, G.A.: 1968, *Astrophys. J.* **151**, 531
Sandage, A., Tammann, G.A.: 1981, *The Revised Shapley-Ames Catalogue of Galaxies*, Carnegie Institution of Washington Publ. *N°* 635
Shostak, G.S.: 1973, *Astron. Astrophys.* **24**, 411
Shostak, G.S., Rogstad, D.H.: 1973, *Astron. Astrophys.* **24**, 405
Sivan, J.-P.: 1977, Thèse de Doctorat d'Etat (Univ. de Provence), Marseille
Sivan, J.-P., Stasińska, G., Lequeux, J.: 1986, *Astron. Astrophys.* **158**, 279
Smith, H.E.: 1975, *Astrophys. J.* **199**, 591
van den Bergh, S.: 1981, *Astron. J.* **86**, 1464
Véron, P., Sauvayre, A.: 1965, *Astron. Astrophys.* **28**, 698
Wevers, B.M.H.R.: 1984, Thesis, University of Groningen

This article was processed by the author using Springer-Verlag TEX AA macro package 1989.